A SINGLE-FILE MODEL FOR POTASSIUM TRANSPORT IN SQUID GIANT AXON

SIMULATION OF POTASSIUM CURRENTS AT NORMAL IONIC CONCENTRATIONS

H.-H. KOHLER, *Institut für Systemdynamik und Regelungstechnik, Universität Stuttgart, D 7 Stuttgart, West Germany*

ABSTRACT A physical model for potassium transport in squid giant axon is proposed. The model is designed to explain the empirical data given by the Hodgkin-Huxley model and related experiments. It is assumed that K^+ moves across the axon membrane by single-file diffusion through narrow pores. In the model a pore has three negatively charged sites that can be occupied alternatively by K^+ or by a gating particle, GP^{++}, coming from the external surface. GP^{++} is considered to be part of the membrane rather than a diffusible component of the surrounding solutions. A high activation barrier for GP^{++} is supposed at the inner membrane border so that it cannot change over to the internal surface. Therefore potassium diffusion can be blocked by GP^{++} penetrating into the pores. This mechanism controls the dynamic behaviour of the model. The time-dependent probabilities of the pore states are described by a system of differential equations. The rate constants in these equations depend on the ionic concentrations, the membrane voltage, and the electrostatic interaction between ions in a single pore. Detailed computational tests for normal composition of external and internal solutions show that the model agrees remarkably well with the stationary and dynamic behaviour of the Hodgkin-Huxley model. However, the hyperpolarization delay is not reproduced. A structural modification, concerning this delay and the way in which GP^{++} is attached to the membrane, is proposed, and the qualitative behavior of the model at varied external and internal concentrations is discussed.

INTRODUCTION

The electrical current during excitation of the squid giant axon is mainly carried by sodium and potassium ions. In the Hodgkin-Huxley model (1) the potassium current is described by

$$I_K = g_K(V - V_K), \tag{1}$$

where V is the membrane voltage (potential difference between inside and outside), V_K the potassium equilibrium voltage, and g_K the (specific) potassium conductance.

Dr. Kohler's present address is: Lehrstuhl für Physikalische Chemie, Universität Regensburg, D 84 Regensburg, W. Germany.

g_K can be written as

$$g_K = \hat{g}_K n^4, \tag{2}$$

where $\hat{g}_K$ is the maximal value of g_K. n is described by a first order process

$$\tau_n(dn/dt) + n = \bar{n}. \tag{3}$$

Both the time constant τ_n and the stationary value $\bar{n}$ are functions of V only. These functional dependences, formulated quantitatively by Hodgkin and Huxley, are shown graphically in Fig. 1.

The Hodgkin-Huxley model is deduced from empirical data. The molecular mechanism of the ionic conductivity changes is still unknown. In this paper a physical model for the potassium conducting system is proposed that will perhaps contribute to a better understanding of this mechanism. The model is based on the assumption that diffusion within the membrane is restricted to single-file pores representing a common diffusion path both for potassium and for gating ions. Single-file pores are narrow channels in which particles jumping from site to site cannot overtake each other. Hence potassium diffusion may be blocked by gating ions penetrating into the pores.

The concept of single-file diffusion was first used by Hodgkin and Keynes (2) to explain deviations from independence in the potassium currents of squid giant axon. From tracer experiments they concluded that a potassium-conducting pore should have an average of about 2.5 occupied sites, to meet the ratio of unidirectional fluxes observed experimentally. Further evidence for single file pores has been found since (3).

BASIC ASSUMPTIONS

The potassium transport system is characterized in detail by the following assumptions: (*a*) Potassium transport takes place through single-file pores independent from each other and with identical physical properties. (*b*) The pores have a marked affinity for potassium and gating ions (GP^{++}). Every pore contains three sites with a negative unit charge fixed to each of them. Each site can be empty or occupied by either one potassium or one gating ion. It follows that a pore can exist in $3^3 = 27$ distinct states. There is a fixed concentration of GP^{++} on the external surface. (*c*) The transition of GP^{++} between pore and internal surface is prevented by a high activation barrier at the inner mouth of the pore.

Because of the last assumption, divalent GP^{++}, coming from the external surface, is increasingly forced into the pores and trapped within them at decreasing membrane voltage. Thus more and more pores will be blocked and fail to contribute to the diffusion of K^+, in qualitative agreement with the Hodgkin-Huxley model (Fig. 1). The model resulting from the assumptions *a* to *c* will be simply called "the pore model" in the following.

In assumption *a* independent pores have been assumed. Cooperativity between

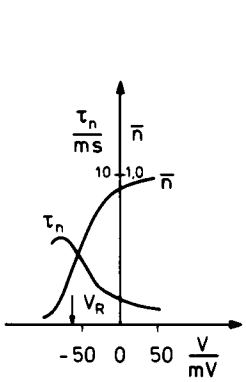

FIGURE 1

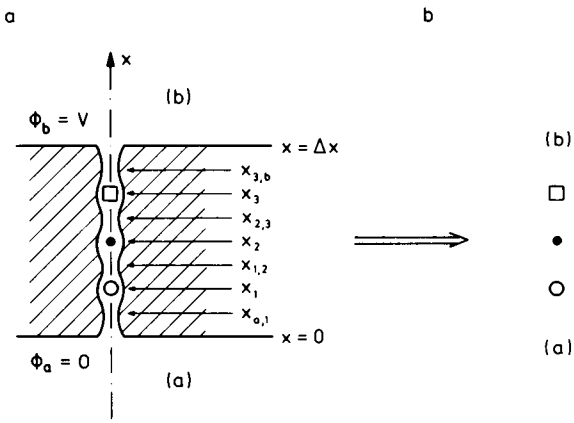

FIGURE 2

FIGURE 1 Time constant τ_n and stationary value $\bar{n}$ vs. membrane voltage V. V_R, membrane resting voltage.

FIGURE 2 *a*. Longitudinal section of a pore, (a), external medium, (b), internal medium, Δx, thickness of axon membrane, x_1, x_2, x_3, position of sites, $x_{a,1}, x_{1,2}, x_{2,3}, x_{3,b}$, position of barriers. See text for further explanation. *b*. Simplified representation of a pore state.

channels is unlikely, since the distance between potassium channels is estimated to be in the order of 10^3 Å (4). Furthermore, computing cooperative models for the squid potassium currents, Hill and Chen find that the time-course of K^+ fluxes cannot be due to cooperativity within and between channels (5, 6). In assumption *b* competition between potassium and gating particles is assumed. As the potassium-conducting pores have to be almost completely filled to be consistent with the ratio of unidirectional fluxes found by Hodgkin and Keynes (2), this competition will be very distinct and greatly influence the performance of the model. For instance, the action of the external voltage V on the gating ions present in a pore is multiplied. For GP^{++} is driven by V, not only because of its own charge, but also because it is pressed in ($V < 0$) or swept out of the pore ($V > 0$) by neighboring potassium ions, which, too, are driven by the external voltage.[1] This "dragging effect" is a typical phenomenon in filled single-file pores. A similar model with Ca^{++} as gating ion has been proposed by Heckmann et al. for the steady-state sodium transport in frog skin epithelium (7). Problems of single-file diffusion, in general, have been treated by Heckmann and by Hill (e.g. 8–10).

It will be shown in the next section that the pore model obeys a system of differential equations of 27th order. This system describes the probabilities p_i (i = state number = 1 ... 27) to observe a pore in the ith state. The rate constants $k_{i,j}$

[1] Fischer, K., K. Heckmann, W. Nonner, and W. Vollmerhaus. Current-voltage curves for porous membranes in the presence of pore-blocking ions. II. Narrow pores containing no more than one vacancy. In preparation.

for transitions from a state i to a state j turn out to be the crucial parameters of the model and are described under "Rate Constants." With reasonable assumptions about the magnitude of the rate constants, the system of differential equations can be lumped to a system of fifth order shown under "Simplified Model Equations." The resulting expression for the current density I_K is easily derived. "Simulations" contains a comparison with the Hodgkin-Huxley model both under stationary and dynamic conditions. On the basis of these results the Discussion section will attempt to give a preliminary answer to the question, whether the pore model, in principle, is compatible with experiments at varied concentrations in external and internal solutions.

MODEL EQUATIONS

In Fig. 2 the longitudinal section of a pore as well as the schematic representation of a pore state are shown. The length of the pore is $\Delta x \approx 100$ Å, the sites are situated at x_1, x_2, x_3, and the barriers at $x_{a,1}$, $x_{1,2}$, $x_{2,3}$, $x_{3,b}$, where $x_{3,b}$ cannot be surmounted by GP^{++}. The diameter of the pore is supposed to be a few Å. $V = \phi_b - \phi_a$ is the membrane voltage, ϕ_b the potential of the internal and ϕ_a of the external medium. Subscript "a" will be generally used for quantities in the external medium or at the external surface, "b" for the internal medium. The occupation of the three sites is denoted by the following symbols: • empty; ○ occupied by K^+; □ occupied by GP^{++}.

In Fig. 3 a number has been assigned to each of the 27 pore states, which are represented schematically at the top of the figure. The lower part of Fig. 3 shows the transition diagram. Here states are represented by points, possible transitions between neighboring states by lines, any line representing transitions in both directions. For example, it can be seen that state 9 changes into state 10 (or simply 9 → 10) if GP^{++} jumps to the central site, that 9 → 13 if K^+ enters from the external medium, and that 9 → 22 if another GP^{++} jumps in. Notice that a GP^{++} on site 3 cannot leave the

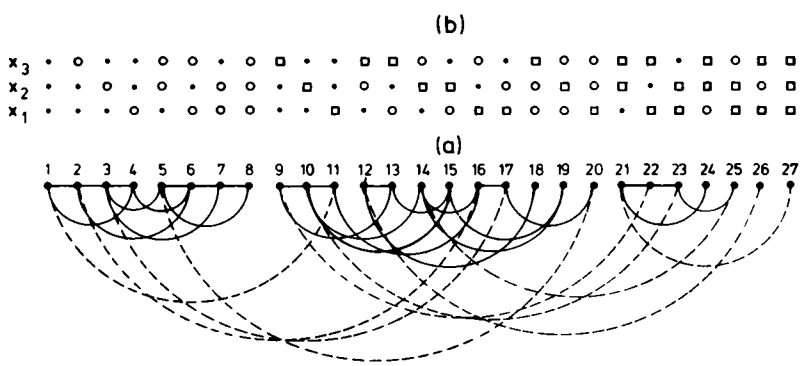

FIGURE 3 Transition diagram. (- - - - -) transition by GP^{++} ions entering or leaving a pore; (——) other transitions.

pore because of assumption *c*, so that there is no line connecting state 9 to state 1 in the diagram.

Let p_i denote the probability to observe a pore in the ith state. The increase per unit time of p_i is given by the difference of probability flows to and from state i. Since the probability flows result from first-order reactions, we find (8)

$$\dot{p}_i = \mathrm{d}p_i/\mathrm{d}t = -\sum_{j \neq i} k_{i,j} p_i + \sum_{j \neq i} k_{j,i} p_j \qquad i = 1, \ldots, 27, \tag{4}$$

where $k_{i,j}$ is the rate constant for transitions from a state i to a state j. It is equal to zero when state i and j cannot be directly converted into each other, that is, when there is no direct connection between these states in Fig. 3.

RATE CONSTANTS

The analytical treatment of the rate constants $k_{i,j}$ will be based on Eyring rate theory (11, 12), the derivation of $k_{19,14}$ may serve as an example. Let us assume, for the present, that the external voltage V is zero. As is seen from Fig. 3, transition 19 → 14 is brought about by K^+ jumping from site 1 over the activation barrier at $x_{a,1}$ (Fig. 2) to the external medium. This transition is influenced by electrostatic interaction of the jumping K^+ with the charges of the other sites and their occupying ions. To give a quantitative description of this interaction, we first regard the theoretical case of an elongated pore, in which the short-range conditions are unchanged, but where distances between surfaces, barriers, and sites are large enough to neglect the electrostatic interaction in question. In this case, the rate constant for a transition of K^+ from site 1 to the external medium is independent of the net charge of the other pore sites. Denoting it by ρ_a^K, we thus have

$$k_{19,14} = \rho_a^K, \tag{5}$$

where ρ_a^K is subscripted by "a" because a jump into the external medium is considered, and by "K" because K^+ is the jumping particle. Shrinking the pore now to its actual length and configuration gives rise to changes of the electrical potential of the jumping particle. Let us denote the potential shifts at barrier and site by $\psi_e(x_{a,1})$ and by $\tilde{\psi}_e(x_1)$. These shifts may be split into additive terms as follows:

$$\begin{aligned} \psi_e(x_{a,1}) &= \phi_e(z_1, z_2, z_3; x_{a,1}) + \phi_K(x_{a,1}), \\ \tilde{\psi}_e(x_1) &= \tilde{\phi}_e(z_1, z_2, z_3; x_1) + \phi_K(x_1). \end{aligned} \tag{6}$$

Here ϕ_k accounts for changes of the self-energy of the potassium ion, due to interaction of this ion with the surrounding solutions (13). ϕ_e arises from bringing the three sites with their respective net valences, z_1, z_2, z_3, into the neighborhood of the barrier at $x_{a,1}$ and at the same time near to the solutions. $\tilde{\phi}_e$, on the other hand, is due to the approach of site 2 and site 3 to site 1, and, again, to the approach of all the three of them to the surrounding solutions. For transition 19 → 14 the net valences are

$$z_1 = -1, \qquad z_2 = 1, \qquad z_3 = 0. \tag{7}$$

Using Eq. 6, Eq. 5 now must be replaced by $k_{19,14} = \rho_a^K \cdot \exp(-(Q_0/kT)\{\phi_K(x_{a,1}) - \phi_K(x_1)\}) \cdot \exp(-(Q_0/kT)\{\phi_e(-1,1,0;x_{a,1}) - \tilde{\phi}_e(1,1,0;x_1)\})$. For $V \neq 0$, there is superposition of an additional potential $\phi(x)$. So, finally, we have

$$k_{19,14} = r_a^K \cdot \exp(-(Q_0/kT)\{\phi_e(-1,1,0;x_{a,1}) - \tilde{\phi}_e(-1,1,0;x_1)\}) \cdot \exp(-(Q_0/kT)\{\phi(x_{a,1}) - \phi(x_1)\}), \tag{8}$$

with

$$r_a^K = \rho_a^K \cdot \exp(-(Q_0/kT)\{\phi_K(x_{a,1}) - \phi_K(x_1)\}). \tag{9}$$

Thus, in Eq. 8, interaction between the jumping particle and the surrounding solutions is contained in r_a^K. The second factor of Eq. 8 accounts for the charge distribution inside the pore, and the third factor for the externally applied voltage. Due to the high ionic strength of the surrounding solutions, the boundary conditions for ϕ_e and ϕ may be approximated by $\phi_e(z_1, z_2, z_3; 0) = \phi_e(z_1, z_2, z_3; \Delta x) = 0$, $\phi(0) = 0$; $\phi(\Delta x) = V$. Assuming that the membrane can be characterized by a relative dielectric constant ϵ_r in the neighborhood of a pore, the method of electrostatic images yields (14, 15)

$$\phi_e(z_1, z_2, z_3; x_{a,1}) = (Q_0/4\pi\epsilon_0\epsilon_r) \sum_{i=1}^{3} \sum_{n=-\infty}^{\infty} \cdot \{z_i/|x_{a,1} - (2n\Delta x + x_i)| - z_i/|x_{a,1} - (2n\Delta x - x_i)|\} \tag{10a}$$

and

$$\phi_e(z_1, z_2, z_3; x_1) = \lim_{x \to x_1} \{\phi_e(z_1, z_2, z_3; x) - (Q_0/4\pi\epsilon_0\epsilon_r) z_1/|x - x_1|\}, \tag{10b}$$

where ϵ_0 is the absolute dielectric constant of free space. $\phi(x)$ is of course a linear function of x. In Fig. 4 the dependence of ϕ_e and ϕ_e on the net valences is illustrated by an example. The value of the dielectric constant and the positions of sites and barrier have been taken from the parameter set used for simulation subsequently.

Expressions analogous to Eq. 8 are readily found for any transition, no matter whether a particle is leaving the pore (as in Eq. 8), entering, or just changing site. Examples for the latter two possibilities are given by the following equations

$$k_{14,19} = \gamma_a^K \cdot \exp(-(Q_0/kT)\phi_e(-1,1,0;x_{a,1})) \cdot \exp(-(Q_0/kT)\phi(x_{a,1})), \tag{11}$$

$$k_{6,5} = s^K \cdot \exp(-(Q_0/kT)\{\phi_e(-1,-1,0;x_{1,2}) - \tilde{\phi}_e(-1,-1,0;x_1)\}) \cdot \exp(-Q_0/kT)\{\phi(x_{1,2}) - \phi(x_1)\}). \tag{12}$$

γ_a^K and s^K are defined in the same sense as r_a^K. We assume that s^K (and accordingly s^{GP} if GP^{++} is the jumping ion) does not depend on the site numbers. $x_{1,2}$ is associated with the barrier between site 1 and 2. γ_a^K is supposed to be proportional to the external potassium concentration, c_a^K.

Assume now that GP^{++} jumps from site 1 to the external surface with the electrical interaction inside the pore determined by either of the two potential profiles of Fig. 4. Then the corresponding rate constants are $k_{25,14}$ and $k_{16,2}$ (see Fig. 3). Their ratio is

$$k_{25,14}/k_{16,2} = \exp(-(2Q_0/kT)\{\phi_e(-1,1,0;x_{a,1}) - \phi_e(-1,-1,0;x_{a,1}) - \tilde{\phi}_e(-1,1,0;x_1) + \tilde{\phi}_e(-1,-1,0;x_1)\}),$$

which would be unity if interaction had been excluded ($\epsilon_r = \infty$), whereas a ratio of 2.7 is calculated from the values in Fig. 4. This example shows that, in the model presented here, electrostatic interaction between charged particles within a pore must not be neglected even if relatively high values of ϵ_r are assumed.

SIMPLIFIED MODEL EQUATIONS

The system of differential equations for the state probabilities (Eq. 4) is of 27th order, so that a significant reduction in order would be very welcome. On account of hydration effects, it may be supposed that ions jumping out of a pore need much higher activation than is necessary for transitions inside a pore. Therefore it may be assumed that the probability of internal hopping from site to site is much higher, both for K^+ and GP^{++}, than the probability of hopping out of the pore. On the other hand, we may assume that K^+ is much more likely to jump out of the pore than GP^{++}. For, on negatively charged sites, the coulombic energy of divalent GP^{++} is much lower than the

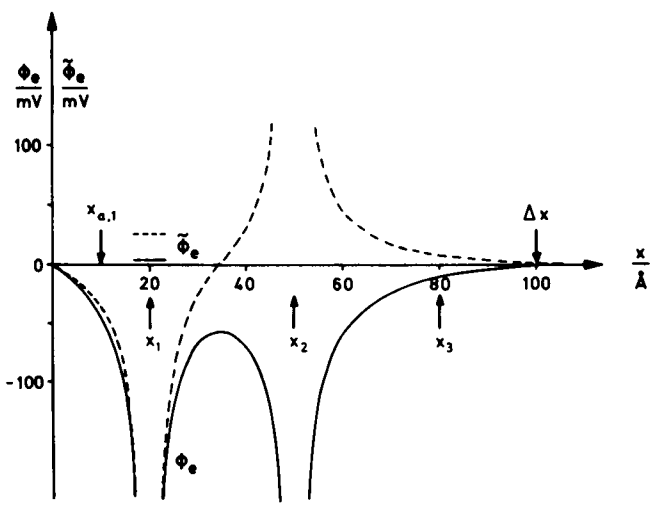

FIGURE 4

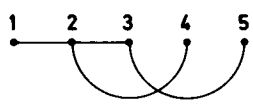

FIGURE 5

FIGURE 4 Electrical potential ϕ_e vs. x for two different choices of net valences, calculated from Eq. 10*a*. Values of $\tilde{\phi}_e$ at site 1 inserted as horizontal lines at $x = x_1$ (Eq. 10*b*). $\epsilon_r = 24$, $x_1 = 20$ Å, $x_2 = 50$ Å, $x_3 = 80$ Å, $x_{a,1} = 10$ Å. (——) $z_1 = -1, z_2 = -1, z_3 = 0$. (- - - -) $z_1 = -1, z_2 = 1, z_3 = 0$.

FIGURE 5 Transition diagram of the reduced system (Eq. 14).

energy of monovalent K^+. Finally if for a given particle the rate constants for hopping out and into a pore are roughly in the same order of magnitude, two clearly separated time domains can be distinguished: domain of slow processes—GP^{++} entering or leaving a pore; domain of fast processes—other transitions.

The dynamic behavior of the system is determined by the slow processes, that is by GP^{++} entering or leaving a pore. These transitions are marked in the diagram of Fig. 3 by dashed lines, whereas the solid lines mark fast transitions. It follows that, with respect to the slow processes, all states connected by solid lines, namely 1–8, 9–20, and 21–25, can be regarded as being in quasi-stationary relation. For example, this means that the probabilities p_1 through p_8 are linked algebraically to V.

Therefore, the dynamic behavior of these probabilities can be expressed by

$$p_i(t) = l_i q_1(t) \qquad i = 1 \ldots 8, \tag{13}$$

where $q_1 = \sum_{i=1}^{8} p_i$ is the compound probability of states 1 through 8 and where the coefficients l_i are functions of the rate constants of the fast processes, so that they depend on V, but not explicitly on time.

Corresponding relations can be established for states 9 through 20 and 21 through 25. Thus, the dynamic behavior of the pore model as a whole can be described by the compound probabilities $q_1 = \sum_{i=1}^{8} p_i$, $q_2 = \sum_{i=9}^{20} p_i$, $q_3 = \sum_{i=21}^{25} p_i$, and the remaining individual probabilities $q_4 = p_{26}$, $q_5 = p_{27}$. To establish the differential equations for the q_i, only transitions along the dashed lines in Fig. 3 need to be considered. So, finally, Eq. 4 reduces to a fifth-order system of the form

$$\mathrm{d}/\mathrm{d}t \begin{bmatrix} q_1 \\ \vdots \\ q_5 \end{bmatrix} = A \begin{bmatrix} q_1 \\ \vdots \\ q_5 \end{bmatrix} \tag{14}$$

which, for convenience, has been written in vector notation.

The elements of matrix A contain the quasi-stationary coefficients l_i, which depend on the rate constants of the fast processes, and the rate constants associated with GP^{++} transitions between pore and external surface. The transition diagram associated with Eq. 14 is shown in Fig. 5. Since there are no cycles, matrix A has nonpositive real eigenvalues. Therefore, under voltage clamp conditions, the time course of the q_i is strictly nonperiodic, as it should be to meet the nonperiodic character of Eq. 3.

Our final interest is in the K^+ current density I_K. Only transitions among states 1 to 8 can contribute appreciably to I_K, because a pore is blocked by GP^{++} in all other states (see Fig. 3). So we find $I_K = NQ_0\{k_{4,1}p_4 + k_{6,2}p_6 + k_{7,3}p_7 + k_{8,5}p_8 - (k_{1,4}p_1 + k_{2,6}p_2 + k_{3,7}p_3 + k_{5,8}p_5)\}$, where N is the number of pores per unit surface. Substituting Eq. 13, we obtain

$$I_K = q_1[NQ_0\{k_{4,1}l_4 + k_{6,2}l_6 + k_{7,3}l_7 + k_{8,5}l_8 - (k_{1,4}l_1 + k_{2,6}l_2 + k_{3,7}l_3 + k_{5,8}l_5)\}]. \tag{15}$$

Denoting the expression in square brackets by $\hat{I}_K$, this simplifies to

$$I_K = q_1 \hat{I}_K. \tag{16}$$

Since q_1 is a probability, we have $0 \leq q_1 \leq 1$. q_1 depends dynamically on V, because it is a solution of Eq. 14; $\hat{I}_K$, on the contrary, is an algebraic function of V. The expression for I_K given by Hodgkin and Huxley happens to have the same basic structure. From Eqs. 1 and 2 we find

$$I_K = n^4 \hat{g}_K (V - V_K), \tag{17}$$

where $\hat{g}_K$ and V_K are constants, and $n = n(V, t)$ with $0 \leq n \leq 1$. Thus, agreement between the pore model and the Hodgkin-Huxley model requires

$$q_1 \stackrel{!}{=} n^4 \tag{18}$$

$$\hat{I}_K \stackrel{!}{=} \hat{g}_K (V - V_K). \tag{19}$$

We call $\hat{I}_K$ the normalized K^+ current density and q_1 the permeability factor. To fulfill Eqs. 18 and 19, the free parameters, contained in the rate constants (r_a^K etc.) and the positions of barriers and sites ($x_{a,1}$, x_1, etc.), have to be fixed appropriately.

SIMULATIONS

The stationary and dynamic features of the pore model and the Hodgkin-Huxley model are compared under voltage clamp conditions. All calculations presented in this section have been made with the following set of parameters:

$T = 279°K$;	temperature
$N = 10^{10} cm^{-2}$;	number of pores per unit surface
$\Delta x = 100$ Å;	thickness of membrane
$\epsilon_r = 24$;	relative dielectric constant
Positions:	
$x_{a,1} = 10$ Å;	barrier between pore and external medium/surface
$x_1 = 20$ Å;	first site
$x_2 = 50$ Å;	second site
$x_3 = 80$ Å;	third site
$x_{3,b} = 100$ Å;	barrier between pore and internal medium
Factors in rate constants:	
$r_a^K = r_b^K = 3.38 \cdot 10^5 s^{-1}$;	associated with K^+ jumping from pore to external/internal medium
$r_a^{GP} = 6.26 s^{-1}$;	associated with Ga^{++} jumping from pore to external surface
$\gamma_a^K = 3.38 \cdot 10^5 s^{-1}$;	associated with K^+ jumping from external medium to pore
$\gamma_b^K = 8.04 \cdot 10^6 s^{-1}$;	associated with K^+ jumping from internal medium to pore
$\gamma_a^{GP} = 21.3 s^{-1}$;	associated with Ga^{++} jumping from external surface to pore.

The precise meanings of r_a^K, r_b^K, r_a^{GP}, γ_a^K, γ_b^K, γ_a^{GP} follow from Eqs. 6 through 12 and from their obvious generalization. s^K, s^{GP}, $x_{1,2}$, etc., do not enter explicitly into cal-

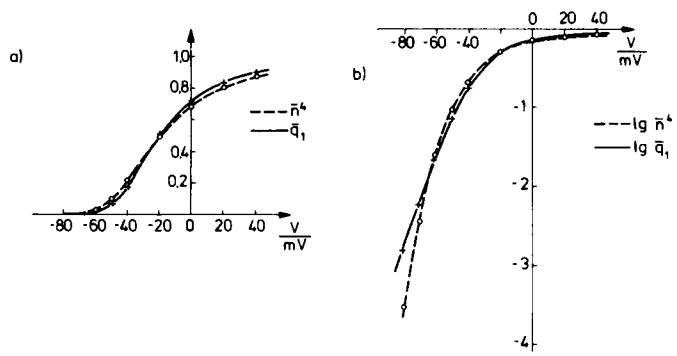

FIGURE 6 Stationary values $\bar{q}_1$ and $\bar{n}^4$ vs. V in (*a*) linear and (*b*) semilogarithmic coordinates.

culations, due to the assumption of quasi-steady states. Therefore, no values have been given to these quantities. Note that the parameter values given above agree with the conditions for quasi-steady states assumed in the preceding section (γ_a^K, γ_b^K, r_a^K, $r_b^K \gg r_a^{GP}$, γ_a^{GP}). The ratio γ_a^K/γ_b^K is identical to the ratio of external and internal potassium concentration.

With the set of parameter values given above, the rate constants $k_{i,j}$, the coefficients l_i (Eq. 13), and matrix A can be computed in successive steps. Then q_1 and I_K are found by the numerical solution of Eqs. 14 and 15.

Stationary Permeability Factor

Let stationary values be marked by horizontal bars. We should have (Eq. 18) $\bar{q}_1 = \bar{n}^4$. Fig. 6 shows that satisfying results are obtained.

Linearity of Instantaneous Currents

If changes in the membrane voltage occur rapidly enough to leave q_1 practically unchanged, I_K is proportional to $\hat{I}_K$ (Eq. 16). Eq. 19 requires $\hat{I}_K = \hat{g}_K(V - V_K)$.

This is approximately fulfilled, as can be seen from Fig. 7. It is evident from Eq. 15 that the linearity of instantaneous currents is not an intrinsic structural quality of the pore model (cf. 11). This is an advantage rather than a deficiency with regard to applications of the pore model to nonphysiological conditions or to other nerve fibers than the squid axon, since most fibers exhibit nonlinear instantaneous currents.

Time-course of the Permeability Factor

We regard the transient of q_1, given by Eq. 14, for voltage steps applied at $t = 0$. Let the voltage be V_0 for $t < 0$ and V for $t > 0$. The time course of q_1 and n, then, is denoted by $q_{1,t}(V, V_0)$ and $n_t(V, V_0)$. Eq. 18 demands that $q_{1,t}(V, V_0) = n_t^4(V, V_0)$. As can be seen from Figs. 8 and 9, this identity is basically fulfilled.

Hyperpolarization Delay

After strong initial hyperpolarization, a considerable delay in the increase of potassium permeability is observed experimentally, which is not incorporated in the Hodgkin-

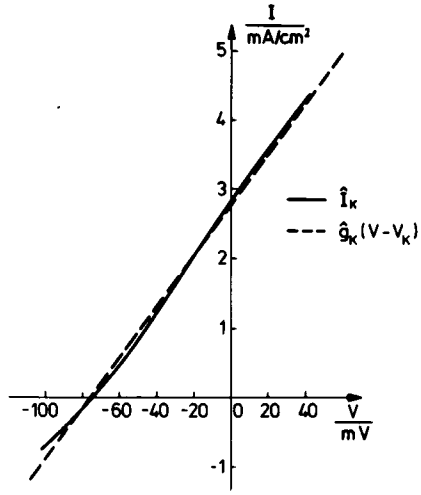

FIGURE 7 Comparison between $\hat{I}_K(V)$ and $\hat{g}_K(V - V_K)$.

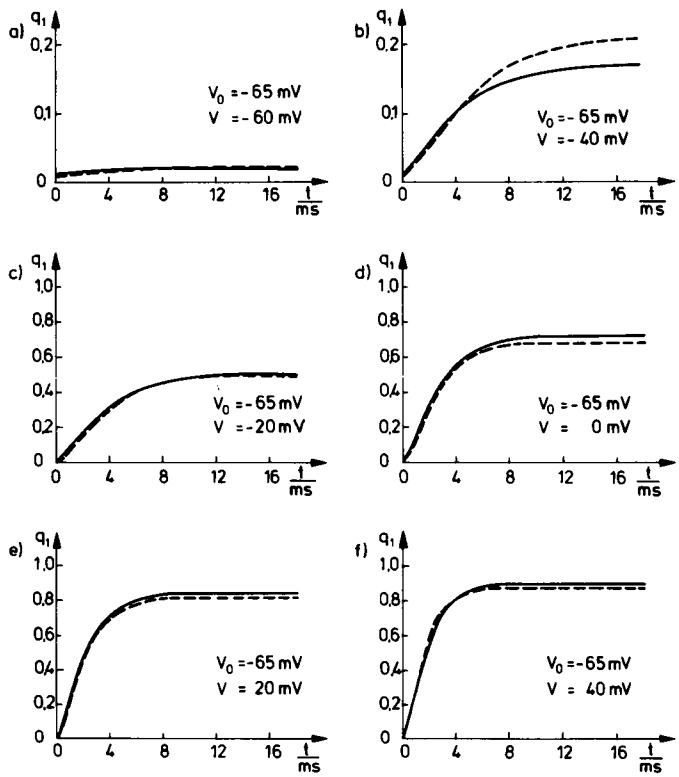

FIGURE 8 Time-course of q_1 and n^4, depolarizing voltage steps. $V_0 = -65$ mV; V increases from a to f. (——) $q_1(t) = q_{1,t}(V, V_0)$; (- - - - -) $n^4(t) = n_t^4(V, V_0)$. See text for further explanation.

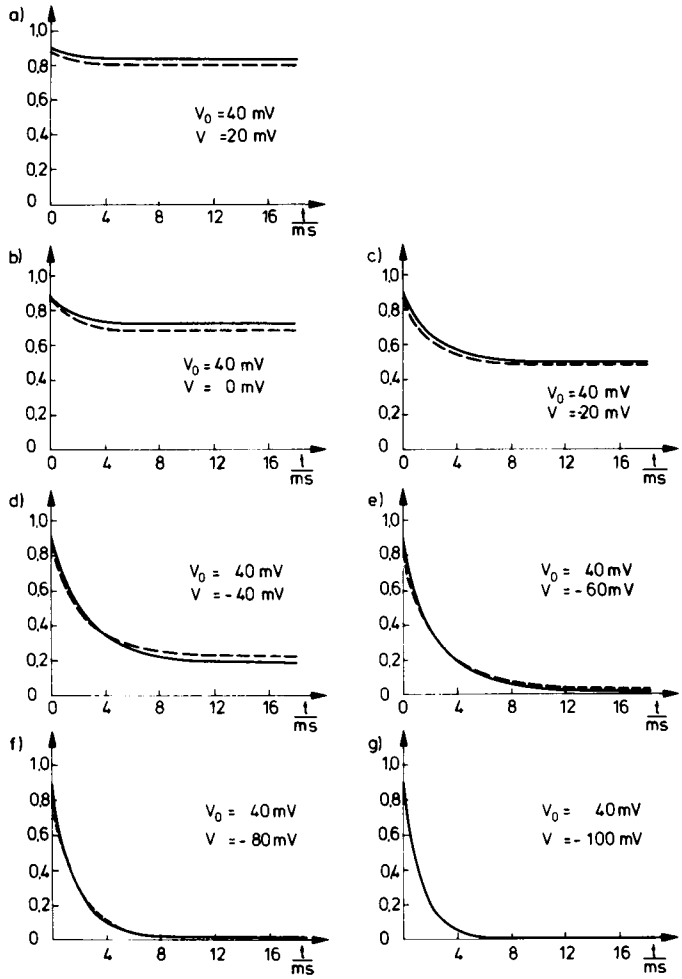

FIGURE 9 Time-courses of q_1 and n^4, repolarizing voltage steps. V_0 = 40 mV; V decreasing from a to g. (——) $q_{1,t}(V, V_0)$; (- - - - -) $n_t^4(V, V_0)$.

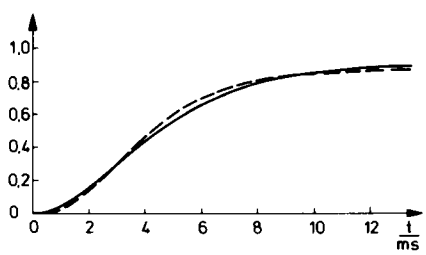

FIGURE 10 Time-course of q_1 and n^4 at depolarization from V_0 = −200 mV to V = 40 mV. (——) $q_{1,t}(V, V_0)$; (- - - - -) $n_t^4(V, V_0)$.

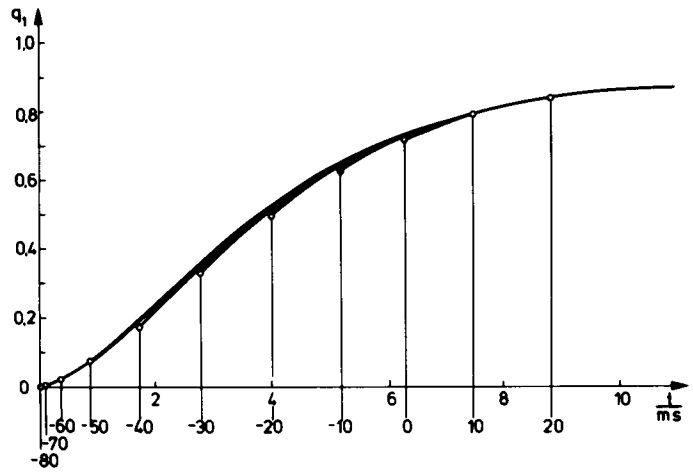

FIGURE 11 Superposition of permeability curves by displacement along the time axis. V_0 (in millivolts) is given at the starting point of the respective curve; V = 40 mV (for all curves).

Huxley model (1, 16). Fig. 10 shows that q_1 and n^4 have nearly identical time-courses, when depolarization to 40 mV is regarded after strong initial hyperpolarization. Hence, the pore model does not produce the hyperpolarization delay either. It can be shown that this failure is of structural origin and cannot be removed by different values of the free parameters.

Superposition

"Superposition" of potassium currents (16) follows immediately from the Hodgkin-Huxley model since n obeys a first-order differential equation (Eq. 3). However, by solving equation 14 for q_1, a fourth-order differential equation is found.

Therefore, in the pore model, superposition is not guaranteed a priori. Yet simulating the measurements of Cole and Moore (16) shows that superposition is well established (Fig. 11). It is surprising that this is true for all values of the free parameters for which tentative computations have been made. Superposition was never perfect, but deviations were not larger than in the original data.

DISCUSSION

In the preceding section it has been shown that the pore model is in good agreement with the Hodgkin-Huxley model, giving satisfactory results for the stationary permeability factor, the linearity of instantaneous currents, the dynamic behavior at voltage clamp, and the superposition of potassium currents. The mean number of K^+ in a potassium-conducting pore is found to be somewhere between 2.2 and 2.3 for -100 mV $\leq V \leq$ 40 mV. This should approximately correspond to the ratio of unidirectional fluxes found by Hodgkin and Keynes (cf. Introduction and ref. 17). The model fails, however, to produce hyperpolarization delay.

In the model the gating particles are assumed to exist as two-dimensional gas on the

membrane surface. The concentration has to be high enough to provide the pores with blocking agents fast enough, even in the case of fast repolarization. The demand for a high concentration of gating particles might be regarded as a shortcoming of the model, for it requires an even higher number of specific surface receptors or surface carriers. This could be avoided by binding the gating particles more closely to the potassium channels. Consider, for instance, pores with negatively charged lateral niches at a distance of about 10 Å from the external surface. Assume that the gating particles withdraw into the niches under more positive voltages and enter from there into the pore when negative voltages are applied. The dynamic and steady-state behavior of such a pore-niche model will differ from the pore model, so that new calculations are necessary. In such a model, however, hyperpolarization delay can be accomplished by a mechanism proposed by Hill and Chen (18). They assume negative charges within the membrane that close the pore by cooperative displacement under hyperpolarization conditions. In our case the charges of the niches might be subject to such a cooperative movement, bringing them quite close to the external surface, so that the niches are deprived of their affinity for the positively charged gating particles. Therefore, at subsequent depolarization, the gating ions have to stay in blocking position within the pore until the negative charges, jumping back into the niches, have restored normal affinity for the gating ions.

Let us return to the pore model in its present form. As mentioned before, conducting pores are nearly filled with potassium ions. So, at $V \ll 0$, the probability of finding site 1 of a conducting pore empty is about inversely proportional to the external potassium concentration and so is, hence, the rate of GP^{++} penetration. This means, at sufficiently negative voltages, that τ_n increases roughly proportional to the external potassium concentration. Such marked increases of τ_n with increasing potassium concentration in fact occur in experiments in which the inactivation of potassium currents, brought about by long-lasting depolarization, is avoided by sufficiently negative holding voltages (19–21).

Hille (22) and Armstrong (3) give detailed accounts of the voltage-dependent block and rectification caused by monovalent ions in the internal solution. They suggest that the inner section of a potassium pore is not very selective, so that other cations than K^+, entering from inside, can jump to the last site and block the pore. Voltage dependence is attributed to two mechanisms. Firstly, the ions may be able to penetrate more or less far into the pore, and, secondly, they are subject to the highly voltage-dependent dragging effect, mentioned under Basic Assumptions, by which they are swept into or cleared of the pore. Evidently, these mechanisms fit very well into the pore model. Simulation of the inactivation phenomena, observed by Armstrong (3, 4) with TEA^+ or other quarternary ammonium ions in the internal solution, will provide another possibility for testing the model under steady-state and dynamic conditions.

Nothing precise can be said at the moment about the chemical nature of the gating ion. Possibly the role of GP^{++} is played by calcium ions coming from the external solution and not from the external membrane surface. This possibility does not affect the mathematical form of the pore model; from the physiological point of view, however,

little is known to confirm or to refute such a calcium plug mechanism. Most experiments concerning the effect of calcium on the potassium currents of squid axon were done with inactivated potassium pores (23, 24), which differ substantially from normal potassium channels both in stationary and dynamic respect. Therefore, to get a clearer picture of the action of both Ca^{++} and K^+ on the potassium conductance of squid axon, detailed experiments in low and high external K^+ and with varying concentration of external Ca^{++} are proposed at negative holding voltages.

Throughout this paper, it was assumed that a pore had three sites. Decreasing the number of sites leads to unsatisfying results. To test the effect of additional sites, calculations with four sites per pore have been carried out. 81 pore states must then be considered. The results, however, apart from better agreement in the hyperpolarization range of Fig. 6, are practically the same as with three sites per pore. Finally, it should be mentioned that the pore model is rather insensitive to the charge of the gating particle. What matters is a high amount of positive charge accumulating near the internal surface of a closed pore. So GP^{++} might be replaced by GP^+ if the number of sites is increased at the same time. Computationally, a lower number of sites is, of course, preferable.

I am indebted to Professor E.D. Gilles and to Professor K. Heckmann for their stimulating discussions.

This work was supported by the Deutsche Forschungsgemeinschaft.

Received for publication 7 September 1976 and in revised form 28 March 1977.

REFERENCES

1. HODGKIN, A. L., and A. F. HUXLEY. 1952. A quantitative description of membrane current and its application to conduction and excitation in nerve. *J. Physiol (Lond.).* **117**:500.
2. HODGKIN, A. L., and R. D. KEYNES. 1955. The potassium permeability of a giant nerve fiber. *J. Physiol. (Lond.).* **128**:61.
3. ARMSTRONG, C. M. 1975. Potassium pores of nerve and muscle membranes. *In* Membranes, A Series of Advances, G. Eisenman, editor. Vol. 3, Marcel Dekker Inc., New York. 325.
4. ARMSTRONG, C. M. 1969. Inactivation of the potassium conductance and related phenomena caused by quarternary ammonium ion injection in squid axon. *J. Gen. Physiol.* **54**:553.
5. HILL, T. L., and Y. CHEN. 1971. On the theory of ion transport across the nerve membrane. II. Potassium ion kinetics and cooperativity (with $x = 4$). *Proc. Natl. Acad. Sci. U.S.A.* **68**:2488.
6. HILL, T. L., and Y. CHEN. 1971. On the theory of ion transport across the nerve membrane. III. Potassium ion kinetics and cooperativity (with $x = 4, 6, 9$). *Proc. Natl. Acad. Sci. U.S.A.* **68**:2488.
7. HECKMANN, K., B. LINDEMANN, and J. SCHNAKENBERG. 1972. Current-voltage curves of porous membranes in the presence of pore-blocking ions. I. Narrow pores containing no more than one moving ion. *Biophys. J.* **12**:683.
8. HECKMANN, K. 1972. Single file diffusion. *In* Biomembranes, Vol. 3, Passive Permeability of Cell Membranes, K. Kreuzer and J. F. G. Slegers, editors. Plenum Publishing Corp., New York. 127.
9. HILL, T. L. 1966. Studies in irreversible thermodynamics. *J. Theor. Biol.* **10**:442.
10. HILL, T. L. 1971. Cooperative effects in models of steady-state transport across membranes. *Biophys. J.* **11**:685.
11. ZWOLINSKI, B. J., H. EYRING, and C. E. REESE. 1949. Diffusion and membrane permeability. *J. Phys. Chem.* **53**:1426.
12. HILL, T. L. 1960. An Introduction to Statistical Thermodynamics. Addison-Wesley Publishing Co., Inc., Reading, Mass. 194.

13. LAEUGER, P., and B. NEUMCKE. 1973. Ion conductance in lipid bilayers. *In* Membranes, G. Eisenman, editor. Vol. 2. Marcel Dekker, Inc., New York. 1.
14. SMYTHE, W. R. 1968. Static and Dynamic Electricity. McGraw-Hill Book Company, New York. 128.
15. SIMONYI, K. 1973. Theoretische Elektrotechnik. VEB Deutscher Verlag der Wissenschaften, Berlin. 290.
16. COLE, K. S., and J. W. MOORE. 1960. Potassium current in the squid giant axon. Dynamic characteristic. *Biophys. J.* **1**:1.
17. HECKMANN, K. 1965. Zur Theorie der "Single File"-Diffusion, II. *Z. Physik. Chem. Neue Folge.* **46**:1.
18. HILL, T. L., and Y. CHEN. 1972. On the theory of ion transport across the nerve membrane. *Biophys. J.* **12**:961.
19. EHRENSTEIN, G., and D. L. GILBERT. 1966. Slow changes of potassium permeability in the squid giant axon. *Biophys. J.* **6**:553.
20. ADELMAN, W. J., and J. P. SENFT. 1968. Dynamic asymmetries in the squid axon membrane. *J. Gen. Physiol.* **51**:102 S.
21. BEZANILLA, F., and C. M. ARMSTRONG. 1972. Negative conductance caused by entry of sodium and cesium ions into the potassium channels of squid axons. *J. Gen. Physiol.* **60**:588.
22. HILLE, B. 1975. Ionic selectivity of Na and K channels of nerve membrane. *In* Membranes, A Series of Advances, G. Eisenman, editor. Vol. 3. Marcel Dekker, Inc., New York. 255.
23. GILBERT, D. L., and G. EHRENSTEIN. 1969. Effect of divalent cations on potassium conductance of squid axons. *Biophys. J.* **9**:447.
24. EHRENSTEIN, G. and D. L. GILBERT. 1973. Evidence for membrane surface charge from measurement of potassium kinetics as a function of external divalent cation concentration. *Biophys. J.* **13**:495.